Proc. Natl. Acad. Sci. USA
Vol. 78, No. 6, pp. 3567–3571, June 1981
Biophysics

Electron microscopy shows periodic structure in collagen fibril cross sections

(x-ray diffraction/optical diffraction/molecular packing)

DAVID J. S. HULMES*†, JEAN-CLAUDE JESIOR†, ANDREW MILLER†, CARMEN BERTHET-COLOMINAS†, AND CHARLOTTE WOLFF†

*Developmental Biology Laboratory, Department of Medicine, Massachusetts General Hospital, Harvard Medical School, Boston, Massachusetts 02114; and †European Molecular Biology Laboratory, Grenoble Outstation, Centre des Etudes Nucleaires de Grenoble, 85X, 38041 Grenoble Cedex, France

Communicated by Jerome Gross, February 13, 1981

ABSTRACT **X-ray diffraction was used to monitor the effects of electron microscope fixation, staining, and embedding procedures on the preservation of the three-dimensional crystalline order in collagen fibrils of rat tail tendon. A procedure is described in which the characteristic 3.8-nm lateral spacing is preserved, with increased contrast, in the diffraction pattern of the embedded fiber. This spacing is correlated with the separation between the tangentially oriented equally spaced lines of density observed in electron microscope ultrathin fibril cross sections of the same material. Optical diffraction of electron micrographs gives an objective measure of the periodicity and suggests that the fibril is composed of concentrically oriented crystalline domains. These observations, when combined with a recent interpretation of the native x-ray diffraction data [Hulmes, D. J. S. & Miller, A. (1979) *Nature (London)* 282, 878–880] suggest a tentative model for the three-dimensional structure of collagen fibrils.**

The one-dimensional or axially projected structure of collagen fibrils is well understood, to the resolution of individual amino acids (1–5), in terms of the modified "quarter stagger" theory for the molecular packing (6, 7). However, the way in which this scheme is extended into three dimensions remains controversial (for review, see refs. 8 and 9). X-ray diffraction from tendon fibers (10–12) indicates three-dimensional crystallinity in the molecular packing although, in some specimens, only the one-dimensional 67-nm (*D*) axial periodicity has been observed (13, 14). Collagen fibrils are somewhat analogous to liquid crystals (15–17), and the one-dimensionally ordered and three-dimensionally ordered phases may correspond to a smectic A → B transition. Several interpretations have been suggested for the near-equatorial (i.e., perpendicular to the fiber axis) crystalline x-ray data (8, 9), but recently both the observed spacings and the general intensity distribution have been accounted for by quasi-hexagonal packing of straight tilted molecules (9, 18). In contrast to most of the tetragonal packing schemes, the quasi-hexagonal model does not require the presence of the rope-like intermediate substructures, a few molecules in cross section, called microfibrils.

Electron microscopy, particularly on negatively stained specimens, indicates that collagen fibrils have a filamentous substructure (19, 20). Filaments have also been observed during *in vitro* collagen fibrillogenesis (21–23). Estimates of filament width vary from 1.5 nm to 4 nm, and so it has been suggested that these filaments correspond to either individual molecules (18, 19) or microfibrils (22, 23). Measurements from the random punctate appearance of ultrathin collagen fibril cross sections have also been used in support of the microfibril hypothesis (24, 25). By definition, a microfibril is a *D*-periodic filament having lateral dimensions no greater than 4 nm. *D*-periodic filaments of the appropriate width have been observed (26) but, because of their unknown depth, unequivocal evidence for the existence of a microfibril is still unavailable, and thus the exact nature of the observed filaments remains obscure. Finally, electron microscopy of freeze-fractured preparations (27–31) or ultrathin sections of either inertly dehydrated (25) or chemically treated (32, 33) tissues indicates a helical filamentous arrangement in collagen fibrils.

To date, no concerted attempt has been made to correlate electron microscopic data with the x-ray diffraction observations that indicate three-dimensional crystallinity in collagen fibrils. So far, there has been no evidence from electron microscopy for long-range lateral order in the native molecular packing. In this paper, we describe the initial results of an extensive joint x-ray diffraction-electron microscopy approach to the problem of the three-dimensional molecular packing. A special fixation, staining, and embedding procedure was devised to provide optimum preservation of the native fibril structure with sufficient contrast for electron microscopy. Ultrathin sections of fibrils prepared in this way show a periodic structure in cross section that can be correlated with the near-equatorial x-ray diffraction data.

MATERIALS AND METHODS

X-ray diffraction was used to monitor structural preservation of the fibrils at each stage of processing for electron microscope ultrathin sectioning. The procedure used to obtain the results described below is as follows. Tendon fibers (diameter ≈100 μm) were dissected from adult (at least 2.5 months) rat tails and used either immediately or after storage at −40°C. Freezing before use did not affect either the x-ray diffraction patterns or the electron microscope observations. The fibers were fixed in 4% formaldehyde (pH 3.6, unbuffered) for 2 hr (12, 34, 35), stained in 1% phosphotungstic acid (pH 2.2, unbuffered) for 1 hr, rinsed briefly in H_2O, and stained in 1% uranyl acetate for 1 hr. The fibers were then dehydrated over a period of 2 hr in graded acetone/H_2O mixtures. Then, either the acetone was exchanged for benzene (36) (1 hr, two changes) followed by Epon/benzene infiltration or Epon/acetone infiltration was carried out directly (33% Epon, 3 hr; 66% Epon, overnight; 100% Epon, overnight). The fixative, stains, and Epon were freshly prepared each time, and all operations were performed at 22°C on unstretched fibers. Specimens were then clamped under tension (strain ≈5%) and polymerized in fresh Epon overnight at 37°C followed by 24 hr at 60°C. Tension removes the visible crimp of the fibers (37) and thus improves orientation for both x-ray diffraction and ultrathin sectioning of the embedded specimens.

The publication costs of this article were defrayed in part by page charge payment. This article must therefore be hereby marked "*advertisement*" in accordance with 18 U. S. C. §1734 solely to indicate this fact.

For x-ray diffraction, the source was an Elliott GX20 rotating anode, and the beam was focused with a mirror-monochromator camera at a specimen-to-film distance of 175 mm. Exposures for the embedded fibers were typically 24–48 hr, and the diffraction patterns were recorded on Kodirex film. Ultrathin sections were cut with a diamond knife on a LKB Ultratome and supported on 400-mesh copper grids that had been previously coated with a thin layer of carbon. Longitudinal sections (i.e., parallel to the fiber axis) were ≈75 nm thick (silver interference color), and cross sections were approximately 40 nm thick (dark grey). The sections were examined without further staining in either a Philips EM300 or a JEOL JEM100B electron microscope with a 20-μm objective aperture. Periodic structures could not be observed in fibril cross sections directly on the electron microscope fluorescent screen but were apparent on the micrographs. Pictures were therefore taken essentially at random, and prolonged exposure to the electron beam was minimized. Magnifications, typically ×50,000–×100,000 on the micrographs, were calibrated by using tactoids of light meromyosin (14.3 nm) and crystals of potassium chloroplatinate (0.69 nm). Image analysis was carried out on the optical diffractometer at the European Molecular Biology Laboratory, Grenoble.

RESULTS

The x-ray diffraction pattern of a native tendon fiber (10–12) is compared with that of a fiber that has been fixed, stained, dehydrated, and embedded according to the above procedure (i.e., immediately before ultrathin sectioning) in Fig. 1. The meridional Bragg reflections (i.e., parallel to the fiber axis and vertical in Fig. 1), which arise from the axial *D* periodicity, are intensified in the embedded specimen, as are the reflections on the characteristic (1/3.8) nm^{-1} row line. The exact spacing of this row line from the embedded specimens depends on the dehydration/infiltration procedure. With acetone alone the spacing is (1/4.3) nm^{-1}, but with acetone and benzene it is (1/3.7) nm^{-1}. Of the remaining native row-line spacings [at ≈(1/2.5) nm^{-1}, (1/1.9) nm^{-1}, (1/1.75) nm^{-1}, (1/1.35) nm^{-1}, and (1/1.26) nm^{-1}], only the (1/2.5) nm^{-1} is faintly visible in Fig. 1*b*. In particular, the intense native reflections in the region of (1/1.3) nm^{-1}, which represent the intermolecular Bragg plane spacings in the quasi-hexagonal lattice (9), have vanished and been replaced by a diffuse equatorial intensity with a maximum at ≈(1/1.9) nm^{-1}.

A longitudinal section of a fiber that gives the x-ray diffraction pattern in Fig. 1*b* is shown in Fig. 2. The periodic asymmetric pattern of 12 transverse dark bands per *D* repeat is characteristic of positive staining and thus corresponds to the distribution of charged amino acid residues (1, 2, 4). The resolution is at least 3.5 nm, as this is the smallest interband separation.

Micrographs were taken of more than 200 different regions in several fiber cross sections. The contrast was generally poor but varied from fibril to fibril, presumably because the density of staining depended on the location of the 40-nm section in the 67 nm (*D*) repeat. At least 20% of the micrographs showed a readily discernible, ordered intrafibrillar structure. Fig. 3 is a particularly good example. Both the large and the small diameter fibrils give an impression of concentric circles or spirals composed of equally spaced, tangentially oriented lines of density separated by ≈4.6 nm.

Optical diffraction was used to provide a more objective measure of the periodicities present in the electron micrographs. The micrographs were scanned with a circular aperture. Dif-

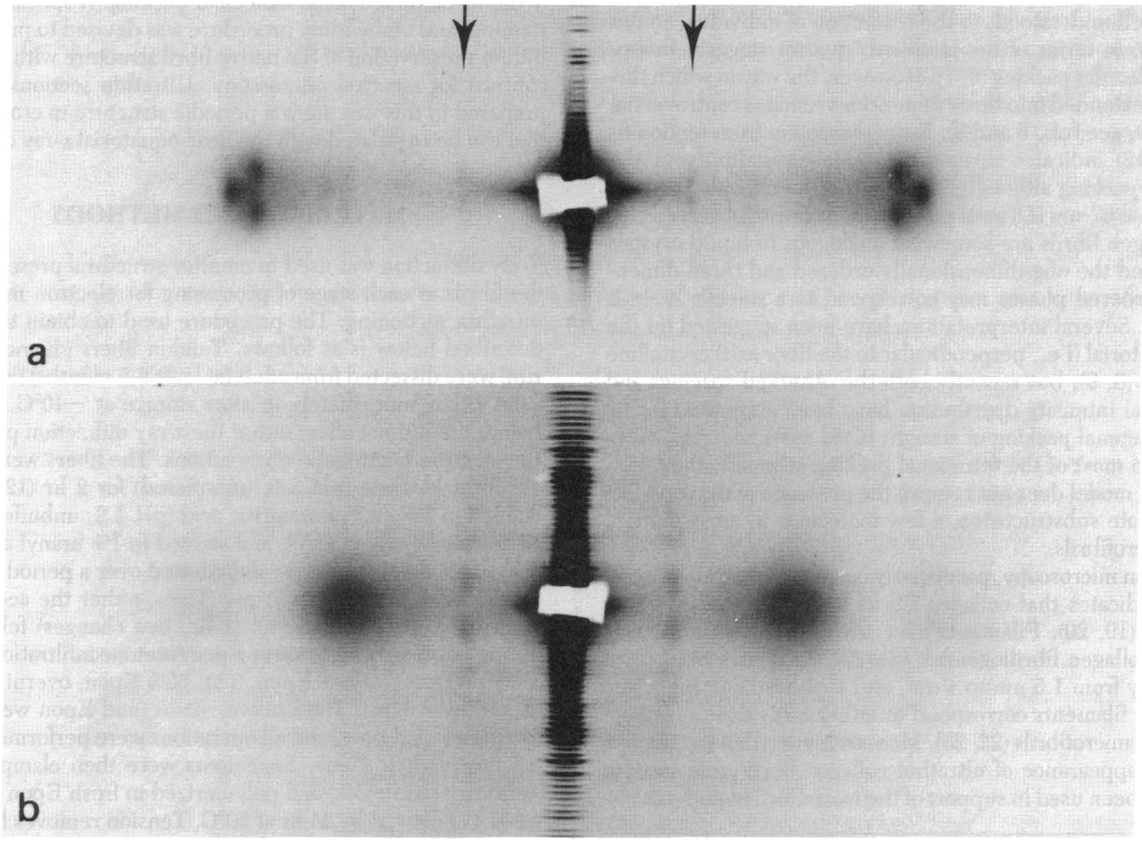

FIG. 1. Medium angle x-ray diffraction patterns of rat tail tendon fibers. Fiber axes vertical. (*a*) Native. (*b*) Embedded. The position of the (1/3.8) nm^{-1} row line is indicated by the arrows. All x-ray and optical diffraction patterns are printed on the same scale.

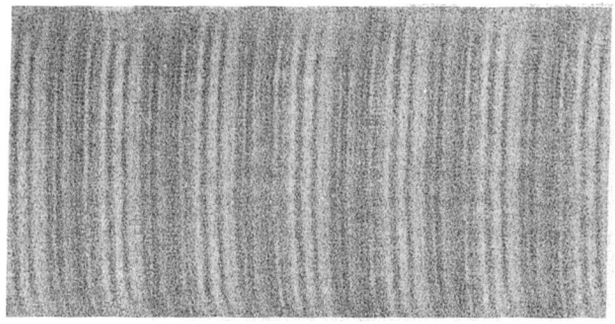

FIG. 2. Longitudinal section showing typical D (67 nm) periodic positively stained banding pattern. (×190,000.)

fraction spots corresponding to periodicities of ≈4.6 nm were consistently obtained (Fig. 4). Optical diffraction analysis on 34 different regions in 13 fibrils gave an average spacing of 4.59 ± 0.28 nm (SD). In all of these observations; (*i*) the periodicity was present in fibril cross sections and not in the interfibrillar space; (*ii*) The diffraction spots were sharp and thus arose from uniformly separated, parallel straight (as opposed to curved) lines in the micrographs; and (*iii*) when areas less than the total fibril cross section were analyzed, the periodicity was consistently detected toward the edge rather than the center of the fibril and, furthermore, the pair of diffraction spots was always oriented perpendicular to the nearest fibril edge, thus indicating that the orientation of the corresponding lines in the micrographs was tangential to this edge.

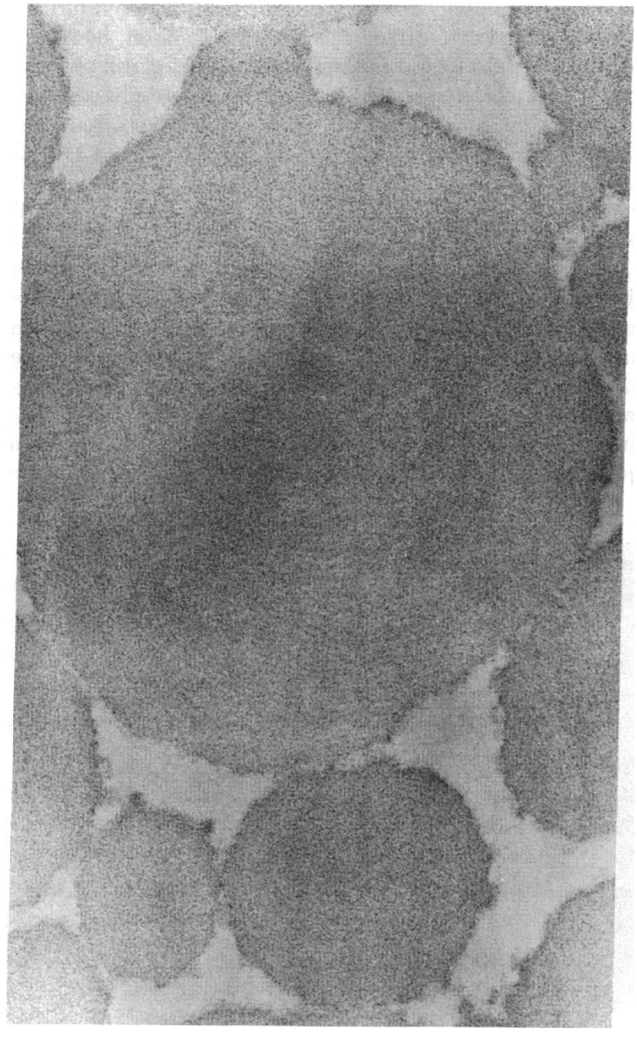

FIG. 3. Transverse section with concentrically oriented lines of density separated by ≈4.6 nm. (×190,000.)

The diameter of the circular aperture used to mask the micrographs was chosen to optimize the signal-to-noise ratio of the optical diffraction spots. Optimal aperture diameters were the equivalent of 120–190 nm on the section, and this is also an approximate measure of the dimensions of the crystalline regions. These figures are consistent with the observed equatorial half-width of the x-ray diffraction reflections from native fibers (10).

By scanning around the center of individual fibril cross sections with optical diffraction, it was possible, in some cases, to follow the angular dependence of the orientation of the (1/4.6) nm^{-1} diffraction spots. Surprisingly, angular variation was accompanied by abrupt changes in the orientations of the spots. Fig. 5, for example, shows optical diffraction patterns from two adjacent areas of the same fibril. In this example, only diffraction spots in the orientations shown were observed in the optical diffraction pattern of the region between the two marked areas. Such abrupt changes in the orientation of the 4.6-nm periodicity are not consistent with the continuous variation that would be expected from either concentric circles or spirals. Instead, the fibril appears to be composed of concentrically oriented domains of crystallinity, with each domain extending ≈100 nm in each lateral dimension.

DISCUSSION

The main conclusions from this work are (*i*) the native, ≈4 nm periodicity has been observed by electron microscopy and (*ii*) this spacing is radially oriented in collagen fibril cross sections.

As pointed out above, the prominent row-line spacing in the x-ray diffraction pattern of the embedded fibers can vary from (1/3.7) nm^{-1} to (1/4.3) nm^{-1}, depending on the dehydration/infiltration procedure. Reflections on this row line remain sharp, however, and the half-width is similar to the half-width of the native (1/3.8) nm^{-1} reflections. The optical diffraction reflections at (1/4.6) nm^{-1} are also sharp and, again, the half-width is similar to the half-width of the native (1/3.8) nm^{-1} reflections. Thus, the extent of long-range order in the electron micrographs is consistent with the x-ray diffraction patterns of the native and embedded fibers. This, and the dimensional variation demonstrated by x-ray diffraction of fixed and embedded specimens, justifies the proposal that the 4.6-nm periodicity detected in the electron micrographs corresponds to the same structural feature as the 3.8-nm periodicity in the native x-ray diffraction pattern. It is possible that there is some swelling in these extremely thin sections as they float on the water surface in the trough of the diamond knife.

Only the two largest native row-line spacing, at ≈(1/3.8) nm^{-1} and (1/2.5) nm^{-1}, are preserved in the x-ray diffraction pattern of the fixed, stained, and embedded fiber. There are a number of possible explanations for this. First, the fixation procedure may be insufficient to preserve the higher resolution features of the native structure. Second, the x-ray diffraction pattern of the embedded fiber will be dominated by the stain distribution. The finite size of the phosphotungstate moiety (35) will limit the resolution to which the stain distribution can accurately represent the molecular packing. Third, the x-ray diffraction intensities depend on the contrast between the electron density of the scattering unit and the electron density of the environment (3). The contrast of collagen embedded in Epon may be lower than the contrast of collagen in an aqueous environment, and this may explain the absence of reflections in

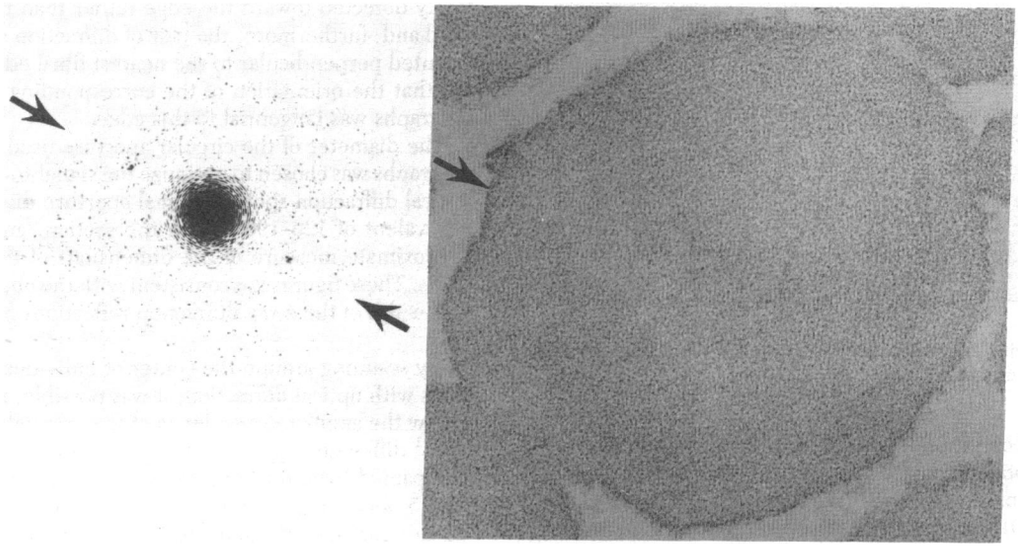

FIG. 4. Transverse section with optical diffraction pattern showing radially oriented 4.5-nm periodicity. For optical diffraction, a circular aperture of effective diameter 190 nm was placed over the fibril near the edge indicated by the arrow. (×200,000.)

the region of (1/1.3) nm^{-1} in the x-ray diffraction pattern of the embedded fiber.

We can offer no satisfactory explanation for the diffuse equatorial intensity at (1/1.9) nm^{-1} in the x-ray diffraction pattern of the embedded fibers (see Fig. 1). Its appearance is associated with phosphotungstic acid staining at low pH (unpublished results; ref. 35) on unstretched specimens. The diffuse intensity indicates short-range order and is of a different character from the sharp (1/3.8) nm^{-1} reflections. Above pH 5, the diffuse intensity is greatly diminished, but the (1/3.8) nm^{-1} row line is relatively intense (35).

Current models for the native crystalline molecular packing differ in that two orthogonal 3.8-nm periodicities are a feature of the tetragonal schemes whereas, in the quasi-hexagonal scheme (9), the 3.8-nm periodicity is present in only one dimension. The latter scheme predicts a 2.5-nm periodicity at ≈75° to the 3.8-nm periodicity. The present electron microscopic observations are consistent with the quasi-hexagonal model; in any one region of the fibril cross section, the 4.6-nm periodicity is present in only one dimension. Without further electron microscopic data in the second dimension, however, definitive evidence for or against either model is still unavailable. Nevertheless, the electron microscope results and the quasi-hexagonal model can be combined to give a tentative model for collagen fibril structure (Fig. 6). There are several interesting features of the model shown in Fig. 6. (*i*) Viewed from the side, the molecules appear tilted by ≈4° to the fibril axis. The direction of tilt is fixed relative to the radially oriented 3.8-nm spacing. Therefore, the molecules appear to follow a "helical" path around the fibril (25, 27–33). Variations in the molecular tilt could be responsible for the observed variation in the *D* period (38–40). (*ii*) Molecules on the fibril surface are in axial register. This may be related to the possible role of segment-long spacing aggregates in fibrillogenesis (41). As the 3.8-nm spacing is oriented radially, the recently reported $n \times 8$-nm quantized increase in fibril diameters (42) would correspond to

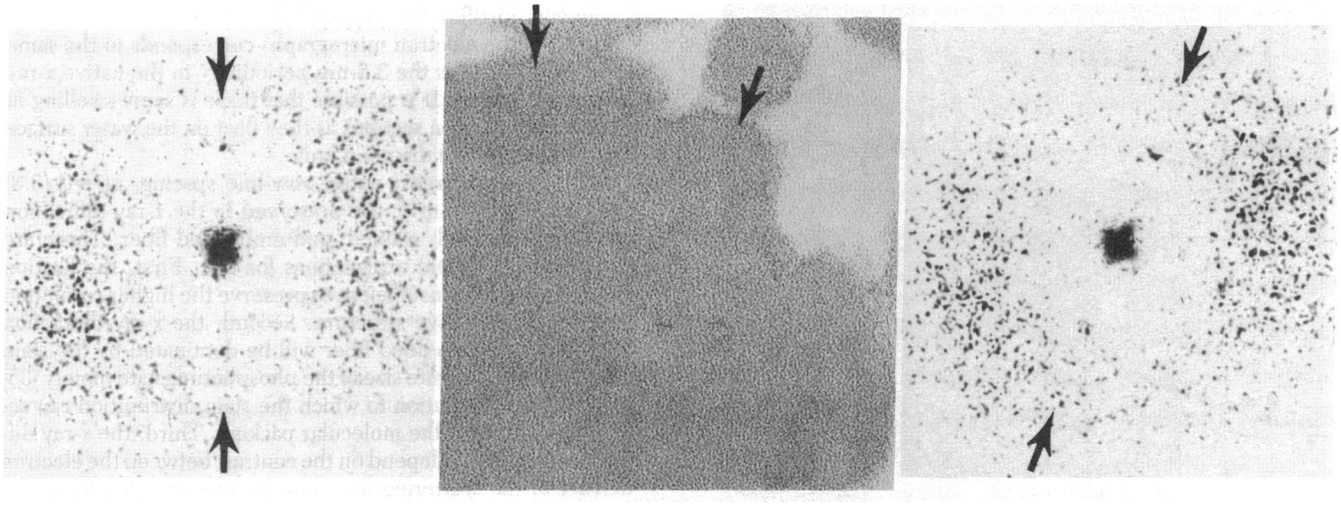

FIG. 5. Transverse section with optical diffraction patterns of adjacent areas (marked by arrows) of the same fibril. The abrupt change in orientation of the ≈(1/4.6) nm^{-1} diffraction spots indicates concentrically oriented crystalline domains. Effective aperture diameter for optical diffraction was 140 nm. (×200,000.)

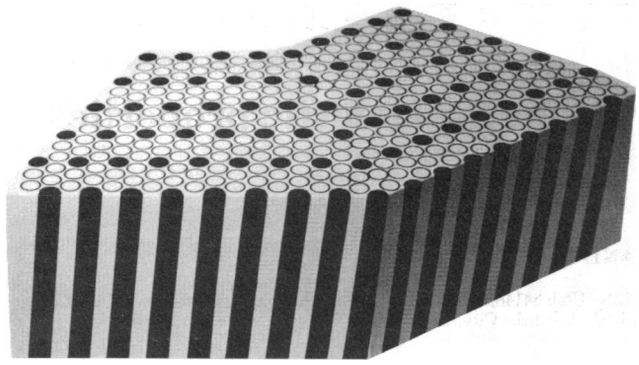

FIG. 6. Perspective view of two adjacent domains in a segment of a tentative model for the three-dimensional molecular packing in collagen fibrils. Open circles indicate sections through individual molecules, and closed circles represent molecular ends; i.e., molecules indicated by open circles are staggered by nD (n = 1, 2, 3, or 4) with respect to the molecules indicated by closed circles. The 3.8-nm spacing is oriented radially and corresponds to the distance between rows of molecular ends. The plane of the molecular tilt is oriented 30° to the exterior surface of each domain.

the addition of a uniform layer, one unit cell thick, of quasi-hexagonal packing around the fibril periphery. (*iii*) Concentrically oriented crystalline domains have also been observed in some forms of microtubule packing (43). Also, domain-like organization of crystallites consisting of hexagonally packed tilted molecules is a common feature of smectic *B*-type liquid crystals (17). Further work is required to elucidate the nature of the apparent domain-like organization in collagen fibrils.

D.J.S.H. is grateful to Drs. R. R. Bruns and J. Gross for helpful advice and encouragement and was supported at different stages of the work by a European Molecular Biology Laboratory Fellowship, U.S. Public Health Service Grants AM3564 and EY02252, and a European Molecular Biology Organization short-term fellowship. This is publication no. 861 of the Robert W. Lovett Memorial Group for the Study of Diseases Causing Deformities.

1. Doyle, B. B., Hulmes, D. J. S., Miller, A., Parry, D. A. D., Piez, K. A. & Woodhead-Galloway, J. (1974) *Proc. R. Soc. London Ser. B* **187**, 37–46.
2. Chapman, J. A. & Hardcastle, R. A. (1974) *Conn. Tiss. Res.* **2**, 151–159.
3. Hulmes, D. J. S., Miller, A., White, S. W. & Brodsky Doyle, B. (1977) *J. Mol. Biol.* **79**, 137–148.
4. Meek, K., Chapman, J. A. & Hardcastle, R. A. (1979) *J. Biol. Chem.* **254**, 10710–10714.
5. Hulmes, D. J. S., Miller, A., White, S. W., Timmins, P. A. & Berthet-Colominas, C. (1980) *Int. J. Biol. Macromol.* **2**, 338–345.
6. Schmitt, F. O., Gross, J. & Highberger, J. H. (1955) *Exp. Cell Res. Suppl.* **3**, 326–334.
7. Hodge, A. J. & Petruska, J. A. (1963) in *Aspects of Protein Structure*, ed. Ramachandran, G. N. (Academic, New York) pp. 289–300.
8. Miller, A. (1976) in *Biochemistry of Collagen*, eds. Ramachandran, G. N. & Reddi, A. H. (Plenum, New York), pp. 85–136.
9. Hulmes, D. J. S. & Miller, A. (1979) *Nature (London)* **282**, 878–880.
10. Miller, A. & Wray, J. S. (1971) *Nature (London)* **230**, 437–439.
11. Miller, A. & Parry, D. A. D. (1973) *J. Mol. Biol.* **75**, 441–447.
12. Nemetschek, Th. & Hosemann, R. (1973) *Kolloid-Z. Z. Polym.* **251**, 1044–1056.
13. Grynpas, M. (1977) *Nature (London)* **265**, 381–382.
14. Hukins, D. W. L. (1977) *Biochem. Biophys. Res. Commun.* **77**, 335–339.
15. Hukins, D. W. L. & Woodhead-Galloway, J. (1977) *Mol. Cryst. Liq. Cryst.* **41**, 33–39.
16. Hukins, D. W. L. & Woodhead-Galloway, J. (1978) *Biochem. Soc. Trans.* **6**, 238–239.
17. Wendorff, J. H. (1978) in *Liquid Crystalline Order in Polymers*, ed. Blumstein, A. (Academic, New York), pp. 1–41.
18. Miller, A. & Tocchetti, D. (1981) *Int. J. Biol. Macromol.* **3**, 9–18.
19. Tromans, W. J., Horne, R. W., Gresham, G. A. & Bailey, A. J. (1963) *Z. Zellforsch. Mikrosk. Anat.* **58**, 798–802.
20. Olsen, B. R. (1963) *Z. Zellforsch. Mikrosk. Anat.* **59**, 184–198.
21. Trelstad, R. L., Hayashi, K. & Gross, J. (1976) *Proc. Natl. Acad. Sci. USA* **73**, 4027–4031.
22. Williams, B. R., Gelman, R. A., Poppke, D. C. & Piez, K. A. (1978) *J. Biol. Chem.* **253**, 6578–6585.
23. Veis, A., Miller, A., Leibovich, S. J. & Traub, W. (1979) *Biochim. Biophys. Acta* **576**, 88–98.
24. Smith, J. W. & Frame, J. (1969) *J. Cell Sci.* **4**, 421–436.
25. Bouteille, M. & Pease, D. C. (1971) *J. Ultrastruct. Res.* **35**, 314–338.
26. Doyle, B. B., Hulmes, D. J. S., Miller, A., Parry, D. A. D., Piez, K. A. & Woodhead-Galloway, J. (1974) *Proc. R. Soc. London Ser. B* **186**, 67–74.
27. Reed, R. (1973) *Int. Rev. Conn. Tiss. Res.* **6**, 257–305.
28. Rayns, D. G. (1974) *J. Ultrastruct. Res.* **48**, 59–66.
29. Stolinski, C. & Breathnach, A. S. (1977) *J. Cell Sci.* **23**, 325–334.
30. Belton, J. C., Crise, N. & Bhatnagar, R. S. (1978) in *Biomolecular Structure and Function*, ed. Agris, P. F. (Academic, New York), pp. 439–445.
31. Ruggeri, A., Benazzo, F. & Reale, E. (1979) *J. Ultrastruct. Res.* **68**, 101–108.
32. Stirtz, T. (1967) *Das Leder* **18**, 193–204.
33. Lillie, J. H., MacCallum, D. K., Scaletta, L. J. & Occhino, J. C. (1977) *J. Ultrastruct. Res.* **58**, 134–143.
34. Brodsky, B., Hukins, D. W. L., Hulmes, D. J. S., Miller, A., White, S. W. & Woodhead-Galloway, J. (1978) *Biochim. Biophys. Acta* **535**, 25–32.
35. Nemetschek, Th., Riedl, H. & Jonak, R. (1979) *J. Mol. Biol.* **133**, 67–83.
36. Bruns, R. R. (1976) *J. Cell Biol.* **68**, 521–538.
37. Gathercole, L. J. & Keller, A. (1978) *Biochim. Biophys. Acta* **535**, 253–271.
38. Gillard, G. C., Merrilees, M. J., Bell-Booth, P. G., Reilly, H. C. & Flint, M. H. (1977) *Biochem. J.* **163**, 145–151.
39. Stinson, R. H. & Sweeny, P. R. (1980) *Biochim. Biophys. Acta* **621**, 158–161.
40. Brodsky, B., Eikenberry, E. F. & Cassidy, K. (1980) *Biochim. Biophys. Acta* **621**, 162–166.
41. Bruns, R. R., Hulmes, D. J. S., Therrien, S. F. & Gross, J. (1979) *Proc. Natl. Acad. Sci. USA* **76**, 313–317.
42. Parry, D. A. D. & Craig, A. S. (1979) *Nature (London)* **282**, 213–215.
43. Tilney, L. G. (1968) *Dev. Biol. Suppl.* **2**, 63–102.